Supporting Information

A Bi-layer TiO_2 Photoanode for Highly Durable, Flexible Dye-sensitized Solar Cells

Jianjian Lin,[a] Yong Peng,[b] Alexander R. Pascoe,[b] Fuzhi Huang,[b] Yi-Bing Cheng,*[b] Yoon-Uk Heo,[c] Andrew Nattestad,*[d] Wanchul Seung,[e] Sung Kyun Kim,[e] Hoon Joon Yoon,[e] Sang-Woo Kim,[e] Yusuke Yamauchi,[f] Shi Xue Dou,[a] and Jung Ho Kim*[a]

[a]*Institute for Superconducting and Electronic Materials (ISEM), Australian Institute for Innovative Materials (AIIM), University of Wollongong, NSW 2522, Australia. E-mail: jhk@uow.edu.au*
[b]*Department of Materials Engineering, Monash University, Melbourne, Victoria 3800, Australia. E-mail: yibing.cheng@monash.edu*
[c]*Graduate Institute of Ferrous Technology, Pohang University of Science and Technology, San 31, Hyoja-Dong, Pohang 790-784, Republic of Korea*
[d]*Intelligent Polymer Research Institute (IPRI), ARC Centre of Excellence for Electromaterials Science, AIIM, University of Wollongong, NSW 2522, Australia. E-mail: anattest@uow.edu.au*
[e]*School of Advanced Materials Science and Engineering, Sungkyunkwan University (SKKU), Suwon 440-746, Republic of Korea.*
[f]*World Premier International (WPI) Research Center for Materials Nanoarchitectonics (MANA), National Institute for Materials Science (NIMS), 1-1 Namiki, Tsukuba , Ibaraki 305-0044, Japan.*

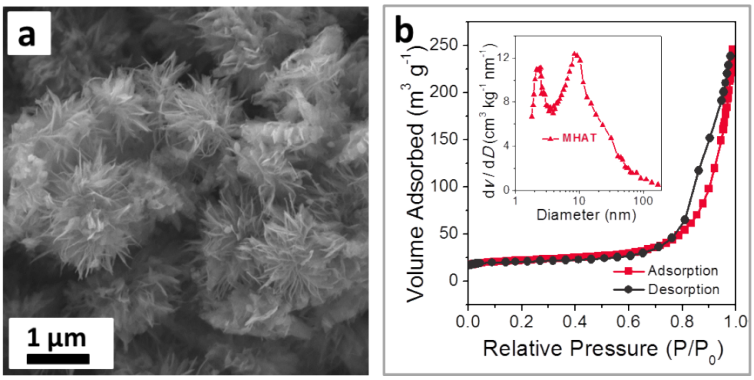

Figure S1. (a) Low magnification FE-SEM image of mesoporous hierarchical anatase TiO_2 (MHAT); (b) N_2 adsorption-desorption isotherm, with the inset image showing the pore size distribution calculated from the adsorption branch of a nitrogen isotherm by the Barrett-Joyner-Halenda (BJH) method.

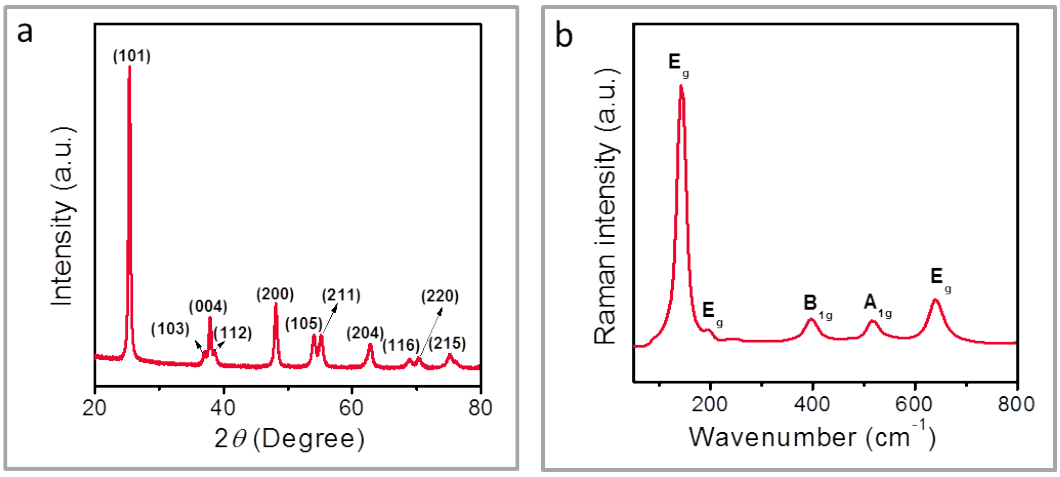

Figure S2. a) XRD pattern of the MHAT, indicating that the spheres are anatase TiO_2 phase (JCPDS No. 21-1272, a = 3.785 Å, b = 3.785 Å, c = 9.514 Å); b) Raman spectrum of the MHAT, confirming the anatase phase from the characteristic Raman modes at 142.1 cm^{-1} (E_g), 194.5 cm^{-1} (E_g), 396.1 cm^{-1} (B_{1g}), 515.8 cm^{-1} (A_{1g}), and 638.4 cm^{-1} (E_g), which can be assigned to the Raman active modes (A_{1g}+B_{1g}+3E_g) of anatase.

Table S1. Photovoltaic characteristics of the DSCs made from P25 and MHAT films with different thicknesses pressed under different applied pressure.

Samples	Pressure (MPa)	Thickness (μm)	J_{sc} (mA cm^{-2})	V_{oc} (mV)	*FF* (%)	η (%)
P25	50	6	5.84	695	58.7	2.39
P25	100	6	5.96	681	59.8	2.43
P25	150	6	7.25	666	65.2	3.15
P25	200	6	7.47	678	65.5	3.32
P25	50	12	7.02	692	65.7	3.19
P25	100	12	7.15	742	67.1	3.56
P25	150	12	8.38	741	65.4	4.06
P25	200	12	9.76	718	64.3	4.50
MHAT	50	6	6.52	716	69.0	3.22
MHAT	100	6	6.56	731	70.7	3.39
MHAT	150	6	6.97	732	69.2	3.53
MHAT	200	6	7.23	751	72.3	3.92
MHAT	50	12	7.24	722	68.7	3.59
MHAT	100	12	8.00	740	71.2	4.22
MHAT	150	12	9.20	720	66.6	4.41
MHAT	200	12	10.90	719	67.3	5.30

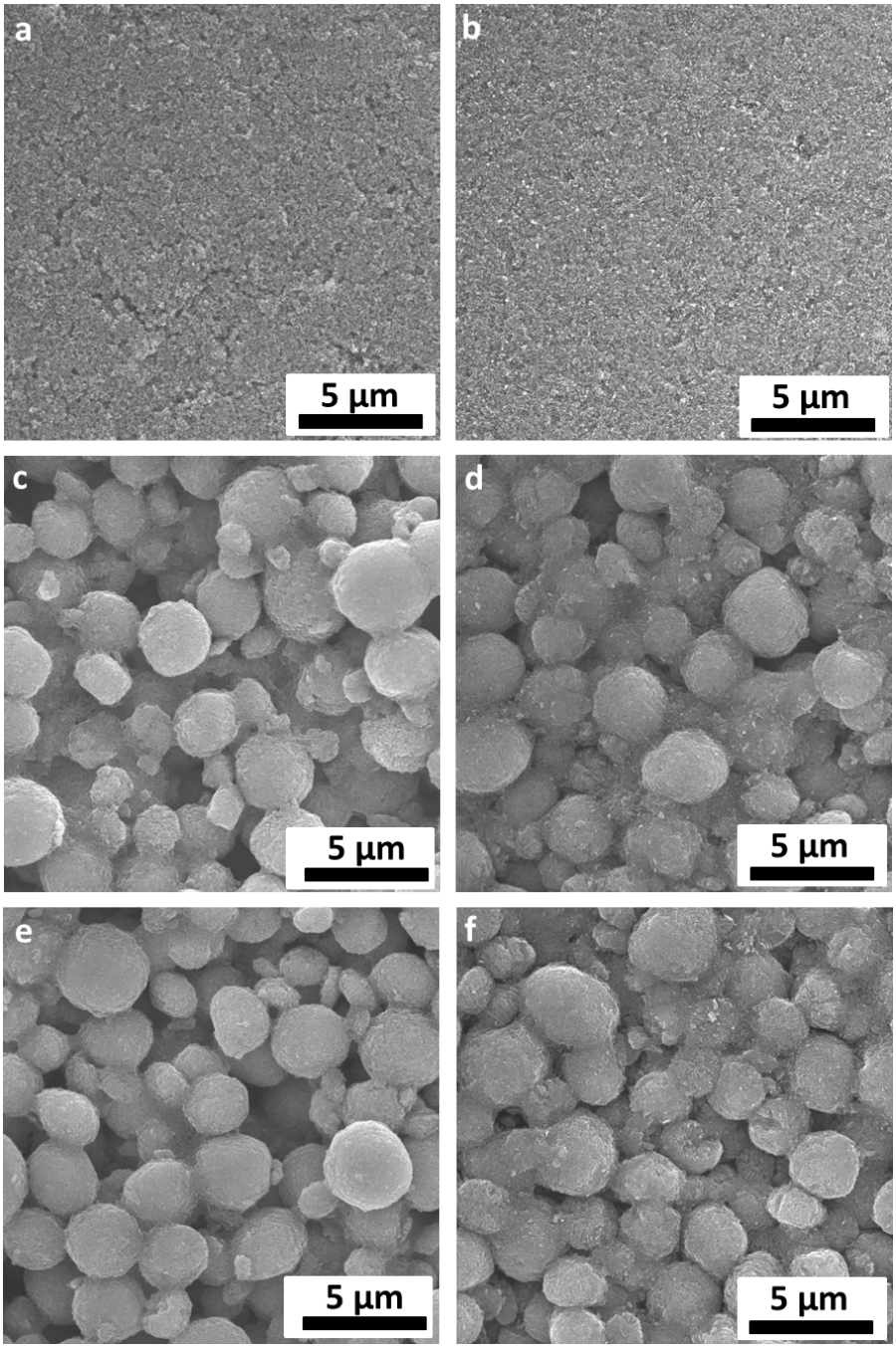

Figure S3. FE-SEM images of different TiO_2 films on ITO/PEN substrate: P25 film (a) before and (b) after CIP; MHAT film (c) before and (d) after CIP; P25/MHAT film (e) before and (f) after CIP.

Table S2. Photovoltaic parameters of DSCs on flexible ITO/PEN substrates based on a MHAT film layer over a P25 under layer (P25/MHAT) before CIP and after CIP (200 MPa), which were measured under air mass (AM) 1.5 global (1.5G) one sun illumination (100 mW cm^{-2}). J_{sc}: short-circuit photocurrent density; V_{oc}: open-circuit photovoltage; *FF*: fill factor; η: total power conversion efficiency. The active areas were ~ 0.16 cm^2 for all of the cells (with the mask area 0.16 cm^2), and the data presented are the average value obtained after testing four cells and finding the standard deviation thereof.

Sample	J_{sc} [mA cm^{-2}]	V_{oc} [mV]	*FF* [%]	η [%]	Thickness[a)] [μm]
P25/MHAT before CIP	8.6 ± 0.3	727 ± 5	64 ± 2	4.0 ± 0.2	12 ± 2
P25/MHAT after CIP	11.7 ± 0.3	733 ± 5	65 ± 2	5.6 ± 0.2	12 ± 2

[a)] Measurement of film thickness was carried out on a surface profile system (Veeco Dektak 150).

Table S3. Photovoltaic parameters of DSCs on flexible ITO/PEN substrates based on a MHAT film layer over a P25 under layer [P25/MHAT ~ 16 μm (12μm P25+ 4μm MHAT)], which were measured under air mass (AM) 1.5 global (1.5G) one sun illumination (100 mW cm^{-2}). J_{sc}: short-circuit photocurrent density; V_{oc}: open-circuit photovoltage; *FF*: fill factor; η: total power conversion efficiency. The active areas were ~ 0.16 cm^2 for all of the cells (with the mask area 0.16 cm^2), and the data presented are the average value obtained after testing four cells and finding the standard deviation thereof.

Sample	J_{sc} [mA cm^{-2}]	V_{oc} [mV]	*FF* [%]	η [%]	Thickness[a)] [μm]
P25/MHAT	11.2 ± 0.3	728 ± 5	64 ± 2	5.2 ± 0.2	16 ± 2

[a)] Measurement of film thickness was carried out on a surface profile system (Veeco Dektak 150).

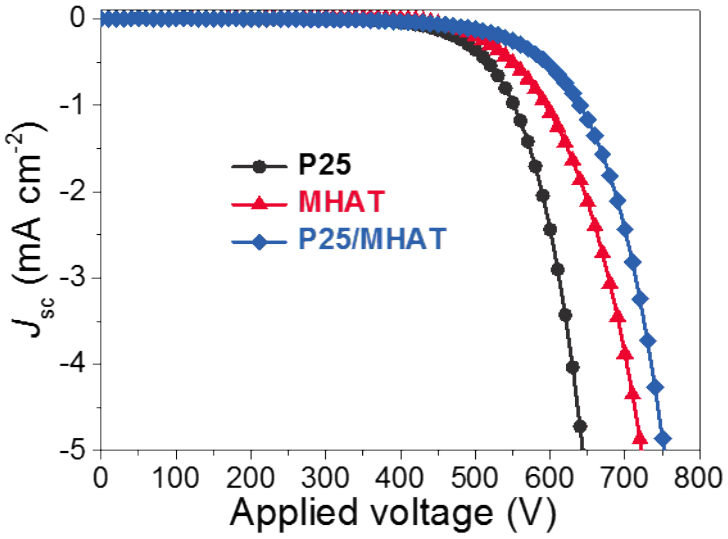

Figure S4. *J-V* characteristics of P25-, MHAT-, P25/MHAT-based flexible DSCs under dark current.

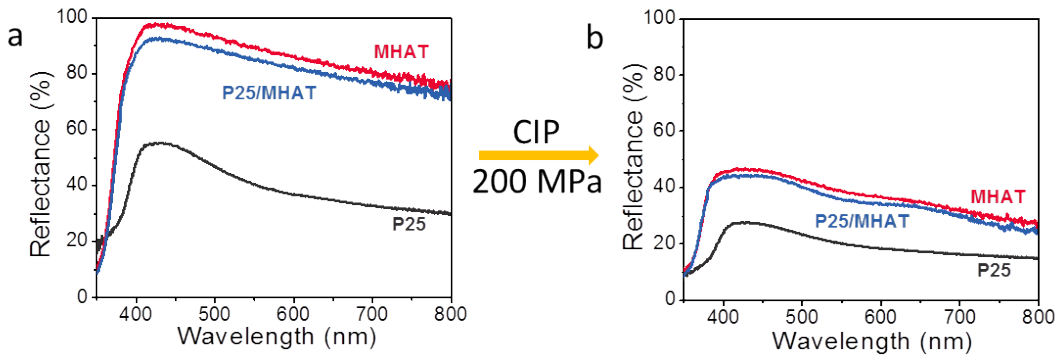

Figure S5. Diffuse reflectance spectra of P25, P25/MHAT and MHAT (a) before and (b) after CIP.

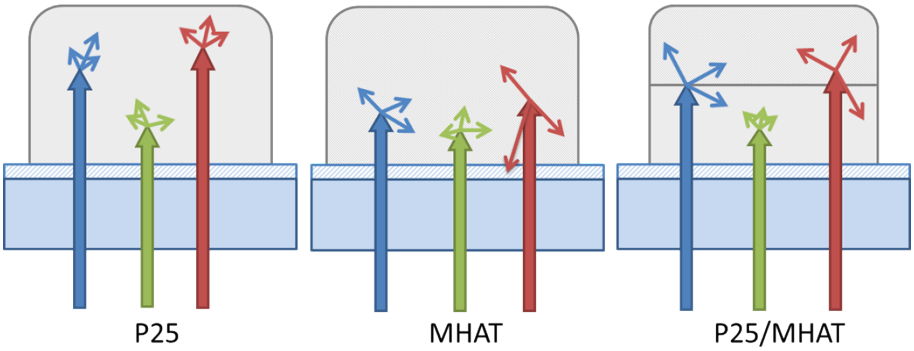

Figure S6. Scheme of light scattering in P25, MHAT, and P25/MHAT films.

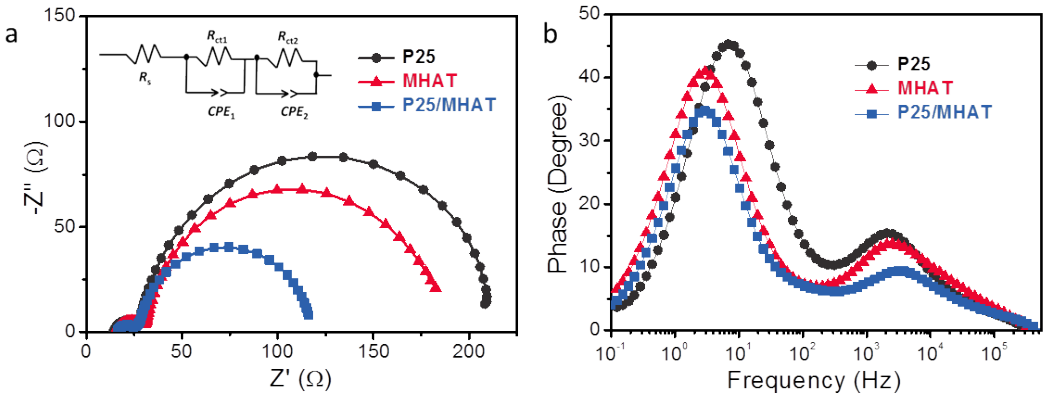

Figure S7. (a) Nyquist plots, with the inset showing the equivalent circuit, and (b) Bode phase plots of flexible DSCs based on P25, MHAT, and P25/MHAT.

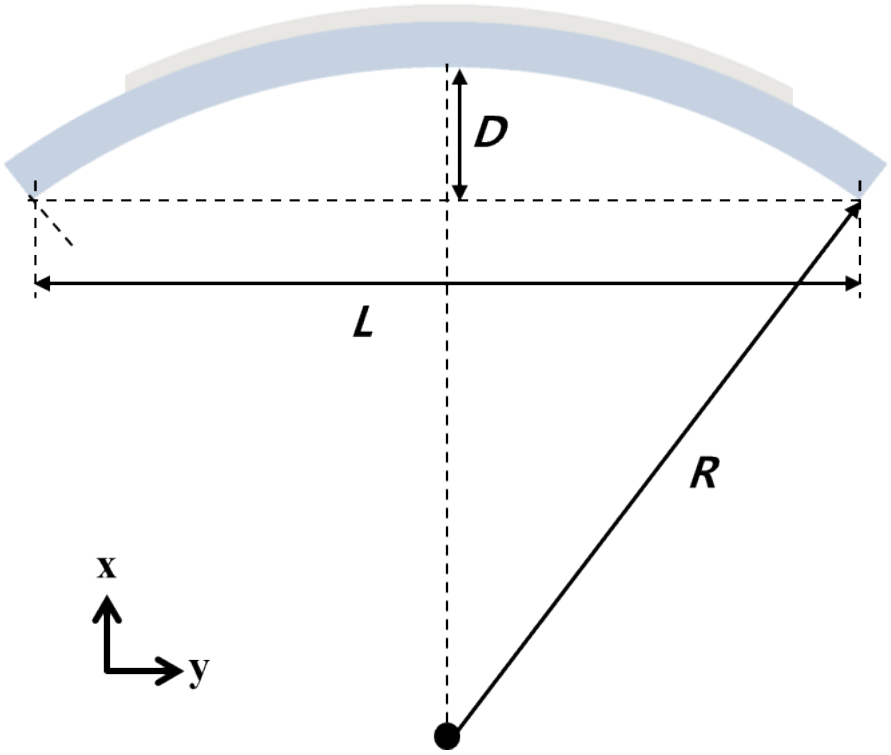

Figure S8. Illustration of bending machine, R can be calculated by the following equation:

$$R = \frac{L^2 + 4D^2}{8D}$$

Where L and D can be measured by ruler during test.[S1]

[S1] B. J. Kim, D. H. Kim, Y.-Y. Lee, H.-W. Shin, G. S. Han, J. S. Hong, K. Mahmood, T. K. Ahn, Y.-C. Joo, K. S. Hong, N.-G. Park, S. Lee, H. S. Jung, *Energy Environ. Sci.* DOI: 10.1039/c4ee02441a.

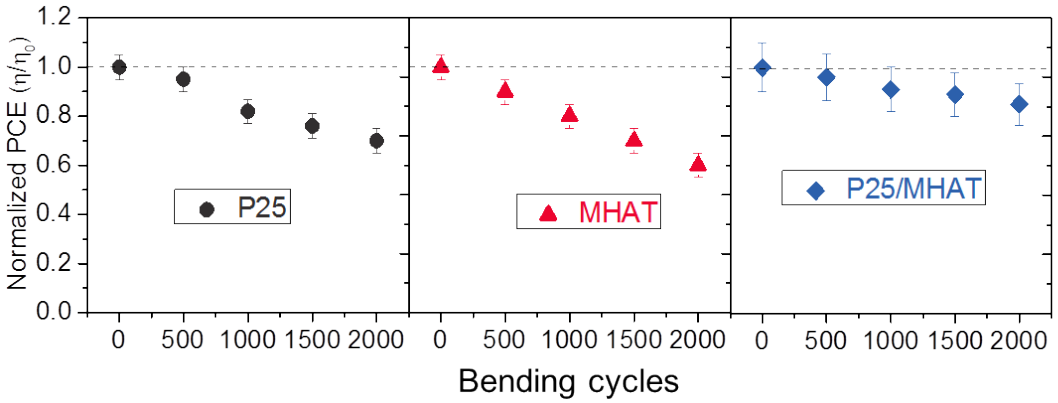

Figure S9. Normalized PCE of P25-, MHAT-, and P25/MHAT-based flexible DSCs as a function of bending cycles, with radius of 50 mm.